

MHD FLOW IN A CHANNEL WITH WAVY POROUS BOUNDARY

D R V PRASADA RAO and R SIVAPRASAD

Department of Mathematics, S K University, Anantapur 515 003

(Received 28 February 1984)

An attempt has been made to study the flow and heat transfer aspect of an incompressible, viscous, electrically conducting fluid in a horizontal porous channel bounded by a wavy wall and a flat wall in the presence of a constant heat source. Using long wave approximation the governing equations of flow and heat transfer have been solved. The influence of heat source, suction and wavyness of the boundaries on the flow has been brought out through the numerical analysis of the velocity, temperature distributions, skin friction and Nusselt number.

Keywords : Heat Transfer ; Wavy porous boundaries

1. INTRODUCTION

HEAT transfer studies with internal heat sources have been proposed for Earth mantle¹⁻³ and for the outer region of star interiors⁴. The volumetric rate of heat generation has been assumed to be either constant⁵⁻⁹ or a function of space variables¹⁰⁻¹⁴. Some authors have considered directly the viscous dissipation and the expansion effect^{15,16}.

In all these investigations the boundaries are assumed to be flat. But there are many physical situations in which the surface of the solid boundaries are wavy in nature. For examples, the surface formed by cleavage of mica contains irregularities of the order of 20A in size, and the irregularities of the surface of an ideally smooth quartz crystal can be up to 100A in height¹⁷. Flow over a wavy wall has attracted the attention of several authors because of its applications in different areas such as transpiration cooling of re-entry vehicles and rocket boosters, cross-hatching on ablative surfaces and film vapourisation in combustion chambers. Keeping this in view, Lekeoudis *et al.*¹⁸ have discussed the viscous flow past wavy walls using linear analysis without restricting the mean flow in the disturbance layer. The effect of wavyness on a viscous flow past an infinite wall has been investigated by Sankar and Sinha¹⁹. Using a perturbation technique similar to Lighthill's method, Vajravelu and sastry²⁰ have extended the above analysis to free convection flow in a vertical wavy channel in the presence of a constant heat source. The hydromagnetic case of this problem has been studied by Rao *et al.*²¹

In this paper an attempt has been made to study the flow and heat transfer aspect of an incompressible, viscous, electrically conducting fluid in a horizontal porous channel bounded by a wavy wall and a flat wall in the presence of a constant

heat source. Using long wave approximation the governing equations of flow and heat transfer have been solved. The influence of heat source, suction and wavyness of the boundaries on the flow has been brought out through the numerical analysis of the velocity, temperature distributions, Skin friction and Nusselt number.

2. FORMULATION AND SOLUTION

Consider the flow of an incompressible, electrically conducting horizontal porous channel bounded below by a flat wall and above by a wavy wall. Choosing the cartesian frame of references $o(x', y')$ such that y' -axis is vertical. Let $y' = 0$ be the lower flat wall and let the wavy wall be represented by $y' = d + \epsilon^* \cos(\lambda'x')$ where ϵ^* the amplitude of the wave, is assumed to be small. A uniform magnetic field of strength H_0 is applied parallel to the y' -axis. The equations governing the steady two-dimensional flow and heat transfer in a viscous incompressible fluid occupying the channel are the momentum equations

$$u' \frac{\partial u'}{\partial x'} + v' \frac{\partial u'}{\partial y'} = - \frac{\partial p'}{\partial x'} + \nu \nabla'^2 u' - \frac{(\sigma \mu_s^2 H_0^2)}{\rho} u' \quad \dots(2.1)$$

$$u' \frac{\partial v'}{\partial x'} + v' \frac{\partial v'}{\partial y'} = - \frac{\partial p'}{\partial y'} + \nu \nabla'^2 v' \quad \dots(2.2)$$

The continuity equation

$$\frac{\partial u'}{\partial x'} + \frac{\partial v'}{\partial y'} = 0 \quad \dots(2.3)$$

and the energy equation

$$\rho c_p \left(u' \frac{\partial T}{\partial x'} + v' \frac{\partial T}{\partial y'} \right) = k \nabla'^2 T + Q \quad \dots(2.4)$$

$$\left(\Delta^2 = \frac{\partial^2}{\partial x'^2} + \frac{\partial^2}{\partial y'^2} \right)$$

where u' and v' are the velocity components, p' is the pressure, σ is the electrical conductivity, μ_s , is the magnetic permeability, c_p is the specific heat at constant pressure, k is the thermal conductivity of the fluid and Q is the constant heat addition/absorption.

The boundary conditions are

$$\left. \begin{aligned} u' = 0, v' = -v_0 (v_0 > 0), T = T_0 \text{ at } y' = 0 \\ v' \cos \phi - u' \sin \phi = -v_0 \cos \phi \\ v' \sin \phi + u' \cos \phi = v_0 \sin \phi \\ T = T_1 \end{aligned} \right\} \text{ on } y' = \eta(x') \quad \dots(2.5)$$

where $\tan \phi = \frac{d\eta}{dx}$ is small.

Defining the non-dimensional variables (x, y, u, v, p, θ) as

$$\begin{aligned} (x, y) &= (x', y')/d, & : & & (u, v) &= \frac{(u', v') d}{\nu} \\ p &= p'/\rho(\nu/d)^2 & : & & \theta &= \frac{T - T_0}{T_1 - T_0} \end{aligned} \quad \dots(2.6)$$

The governing equations and the boundary conditions in the non-dimensional form reduce to

$$\left. \begin{aligned} u \frac{\partial u}{\partial x} + v \frac{\partial u}{\partial y} &= - \frac{\partial p}{\partial x} + \nabla^2 u - M^2 u & \dots(2.7) \\ u \frac{\partial v}{\partial x} + v \frac{\partial v}{\partial y} &= - \frac{\partial p}{\partial y} + \nabla^2 v & \dots(2.8) \end{aligned} \right\}$$

$$\frac{\partial u}{\partial x} + \frac{\partial v}{\partial y} = 0 \quad \dots(2.9)$$

$$P \left(u \frac{\partial \theta}{\partial x} + v \frac{\partial \theta}{\partial y} \right) = \nabla^2 \theta + \alpha \quad \dots(2.10)$$

$$\begin{aligned} u = 0; v = -S; \theta = 0 & \quad \text{on } y = 0 \\ \left. \begin{aligned} v \cos \phi - u \sin \phi &= -S \cos \phi \\ v \sin \phi + u \cos \phi &= S \sin \phi \\ \theta &= 1 \end{aligned} \right\} \text{ on } y = \eta(x) \end{aligned} \quad \dots(2.11)$$

where

$$M^2 = \frac{\sigma \mu_0^2 H_0^2 d^2}{\rho \nu}, \quad \text{the Hartmann number}$$

$$P = \mu(c_p)/k, \quad \text{the Prandtl number}$$

$$\alpha = Qd^2/k(T_1 - T_0), \quad \text{the heat source parameter}$$

$$\epsilon = \frac{\epsilon^*}{d}, \quad \text{the amplitude parameter}$$

$$\lambda = \lambda' d, \quad \text{the frequency parameter}$$

Using the perturbation method we write the total velocity and total temperature distributions as

$$\left. \begin{aligned} u(x, y) &= u_0(y) + \epsilon u_1(x, y) + \dots \\ v(x, y) &= -S + \epsilon v_1(x, y) + \dots \\ p(x, y) &= p_0(x) + \epsilon p_1(x, y) + \dots \\ \epsilon(x, y) &= \theta_0(y) + \epsilon \theta_1(x, y) + \dots \end{aligned} \right\} \quad \dots(2.12)$$

$(u_0(y), -S), \theta_0(y)$ and $p_0(x)$ are the velocity distributions, temperature distribution and applied pressure of mean flow. $(u_1, v_1), \theta_1, p_1(x, y)$ are the perturbations over the velocity, temperature and pressure distributions respectively due to waviness of the boundary substituting (2.12) in equations (2.7)–(2.10) and equating the like powers of ϵ we get

$$\frac{d^2 u_0}{dy^2} + S \frac{du_0}{dy} - M^2 u_0 = c \tag{2.13}$$

$$\frac{d^2 \theta_0}{dy^2} + (PS) \frac{d\theta_0}{dy} = -\alpha \tag{2.14}$$

to the zeroth order and

$$u_0 \frac{\partial u_1}{\partial x} + v_1 \frac{du_0}{dy} - S \frac{du_1}{dy} = -\frac{\partial p_1}{\partial x} + \nabla^2 u_1 - M^2 u_1 \tag{2.15}$$

$$u_0 \frac{\partial v_1}{\partial x} - S \frac{\partial v_1}{\partial y} = -\frac{\partial p_1}{\partial y} + \nabla^2 v_1 \tag{2.16}$$

$$\frac{\partial u_1}{\partial x} + \frac{\partial v_1}{\partial y} = 0 \tag{2.17}$$

$$P \left(u_0 \frac{\partial \theta_1}{\partial x} - S \frac{\partial \theta_1}{\partial y} + v_1 \frac{\partial \theta_0}{\partial y} \right) = \nabla^2 \theta_1 \tag{2.18}$$

to the first order, where $c = \frac{\partial p_0}{\partial x}$.

Assuming the slope of the wavy wall $\left(\frac{d\eta}{dx}\right)$ to be small with the help of (2.12) the boundary conditions (2.11) can be simplified to

$$\left. \begin{aligned} u_0 = 0; \theta_0 = 0 \quad \text{on } y = 0 \\ u_0 = 0; \theta_0 = 1 \quad \text{on } y = 1 \end{aligned} \right\} \tag{2.19}$$

$$\left. \begin{aligned} u_1 = 0; v_1 = 0; \theta_1 = 0 \quad \text{on } y = 0 \\ u_1 = -\exp(i\lambda x) u'_0; v_1 = 0; \theta_1 = -\theta'_0 \exp(i\lambda x) \quad \text{on } y = 1 \end{aligned} \right\} \tag{2.20}$$

where a prime denotes differentiation w.r.t. y . Introducing the stream function $\bar{\psi}_1$ as

$$u_1 = -\frac{\partial \bar{\psi}_1}{\partial y}; v_1 = \frac{\partial \bar{\psi}_1}{\partial x}$$

into (2.15) and (2.16) and eliminating the non-dimensional pressure p_1 , we get

$$\begin{aligned} u_0 \bar{\psi}_{1,x} - u_0 (\bar{\psi}_{1,xyy} + \bar{\psi}_{1,xxx}) + S (\bar{\psi}_{1,yyy} + \bar{\psi}_{1,xyz}) + \\ 2\bar{\psi}_{1,xyy} + \bar{\psi}_{1,xxx} + \bar{\psi}_{1,yyyy} - M^2 \bar{\psi}_{1,yy} = 0 \end{aligned} \tag{2.21}$$

$$P(u_0 \theta_{1,x} - S \theta_{1,y} + \theta'_0 \bar{\psi}_{1,s}) = \theta_{1,ss} + \theta_{1,vy} \quad \dots(2.22)$$

keeping in view the conditions (2.20), we write the general solutoin for $\bar{\psi}$ under the long wave approximation ($\lambda \ll 1$) as

$$\bar{\psi}(x, y) = \sum_i (\lambda^i \psi_i) \exp(i\lambda x) \quad \dots(2.23)$$

$$(i = 0, 1, 2, \dots)$$

Substituting (2.23) in (2.21) and (2.22) and separating the terms of various orders in λ , we obtain the following differential equations to the order of ϵ^2 ,

$$\psi'_0 \circ + S \psi''_0 = M^2 \psi'_0 = 0 ; t'_0 + S P t'_0 = 0 \quad \dots (2.24)$$

$$\left. \begin{aligned} \psi'_1 \circ + S \psi''_1 - M^2 \psi'_1 &= i(u_0 \psi'_0 - u'_0 \psi_0) \\ t'_1 + S P t'_1 &= i P (u_0 t_0 + \theta'_0 \psi_0) \end{aligned} \right\} \dots(2.25)$$

$$\left. \begin{aligned} \psi'_2 \circ + S \psi''_2 - M^2 \psi'_2 &= 2\psi'_2 \circ + S \psi'_0 + i(u_0 \psi'_1 - u'_1 \psi_1) \\ t'_2 + P S t'_2 &= t_0 + i P (u_0 t_1 + \theta'_0 \psi_1) \end{aligned} \right\} \dots(2.26)$$

The boundary conditions (2.20) in terms of ψ_i are

$$\left. \begin{aligned} \psi_0 = 0 ; \psi'_0 = 0 ; t_0 = 0 \quad \text{on } y = 0 \\ \psi_0 = 0 ; \psi'_1 = u'_0 ; t_1 = -\theta'_0 \quad \text{on } y = 1 \end{aligned} \right\} \dots(2.27)$$

$$\left. \begin{aligned} \psi_i = 0 ; \psi'_i = 0 ; t_i = 0 \quad \text{on } y = 0 \\ \psi_i = 0 ; \psi'_i = 0 ; t_i = 0 \quad \text{on } y = 1 \end{aligned} \right\} \text{for } i \geq 1 \quad \dots(2.28)$$

Solving the equations (2.13) and (2.14) using the conditions (2.19), we obtain the mean flow solution as

$$u_0(y) = \frac{c}{M^2} \left[1 + \frac{(\sinh m(y-1) - \exp(S/2) \sinh(my)) \exp(-Sy/2)}{\sinh m} \right]$$

$$\theta_0(y) = c_2(\exp(-PSy) - 1) - a_{40}y$$

where

$$m = \frac{(S^2 + 4M^2)^{1/2}}{2} ; a_{40} = \alpha/PS ; c_2 = \frac{(1 + a_{40})}{(\exp(-PS) - 1)}$$

The perturbed flow solutions in terms of ψ and θ_1 are obtained by solving (2.15)-(2.18) using the conditions (2.20) which are given by

$$\psi_0 = A_1 + A_2y + [A_3 \cosh(my) + A_4 \sinh(my)] \exp(-Sy/2)$$

$$\psi_1 = i(B_1 + B_2(y) + [B_3 \cosh(my) + B_4 \sinh(my)] \exp(-Sy/2) + \phi_1(y))$$

$$t_0 = c_4 (\exp(-SPy) - 1)$$

$$t_1 = i(D_1 + D_2 \exp(-SPy) + \phi_2(y))$$

The perturbed velocity components u_1 , v_1 and temperature θ_1 are given by

$$u_1 = -[\psi'_r \cos(\lambda x) - \psi'_i \sin(\lambda x)]$$

$$v_1 = -\psi_r [\sin(\lambda x) + \psi_i \cos(\lambda x)]$$

and

$$\theta_1 = t_r \cos(\lambda x) - t_i \sin(\lambda x)$$

where

$$\psi_r + i\psi_i = \psi; \quad \psi'_r + i\psi'_i = \psi'$$

$$t_r = i t_i = t; \quad t'_r + i t'_i = t'$$

3. SKIN FRICTION AND HEAT TRANSFER CO-EFFICIENT (NUSSLETT NUMBER) AT THE WALLS

The shear stress τ_{xy} at any point in the fluid is given by $\tau'_{xy} = \mu \left(\frac{\partial u'}{\partial y'} + \frac{\partial v'}{\partial x'} \right)$ which in the dimensionless form reduces to $\tau_{xy} = h^2 \tau'_{xy} / \rho v^2 = \frac{\partial u}{\partial y} + \frac{\partial v}{\partial x}$. At the wavy wall and at the flat wall, τ_{xy} becomes

$$\left. \begin{aligned} \tau_w &= u'_0(1) + \epsilon [(u'_0(1) - \psi'_0(1) \cos(\lambda x) + \lambda \psi'_1 \sin(\lambda x))] \\ \tau_0 &= u'_0(0) + \epsilon [(\psi'_0(0) \sin(x) - \psi''_0(0) \cos(\lambda x))] \end{aligned} \right\} \dots(3.1)$$

The heat transfer co-efficient N' is defined as

$$N' = -k \frac{\partial T}{\partial y}$$

which in non-dimensional form reduces to

$$N = -\frac{\partial N'}{k(T_1 - T_0)} = \frac{\partial \theta}{\partial y}$$

At the wavy wall and flat wall, (3.1) takes the form

$$N_w = \theta'_0(1) + \epsilon [(\theta''_0(1) + t'_0(1) \cos(\lambda x) - \lambda t'_0(1) \sin(\lambda x))]$$

$$N_0 = \theta'_0(0) + \epsilon [t'_0(0) \cos(\lambda x) - t'_1(0) \sin(\lambda x)]$$

4. DISCUSSION

We follow the convention that the fluid region in one half of the channel bounded by the plane wall denotes region I and the remaining half bounded by the wavy wall denotes region II. The profiles for zeroth order axial velocity (u_0) (Fig. 1) are asymmetric bell shaped curves with the maximum attained in the mid plane. The magnitude of the velocity u_0 is general at any point in the region I is large in compared to its magnitudes in region II. For an increase in the Hartmann number M , the velocity u_0 decays rapidly and the decay in the region II is less rapid compared to its decay in the region I. Also it can be observed that when the suction parameter reverse its sign from positive to negative, the velocity in the region I decreases while the velocity near the wavy wall increases. Keeping M fixed, for an increase in suction parameter $S(> 0)$, the axial velocity u_0 increase uniformly in the region I and decreases in the region II. This shows that an increase in the suction parameter $S(> 0)$, causes an increase in the flux in the region I along the channel while an increase in S through negative values causes an increase in flux in the region II.

The zeroth order temperature profiles are drawn in (Figs. 2, 3) for different values of S , α and P . In either case, the temperature grows rapidly in the region I till it attains its maximum in the other half of the channel near the mid plane and then rapidly falls towards the wavy boundary to attain its prescribed value. In case of water ($P = 0.71$) for positive values of suction parameter the growth of the

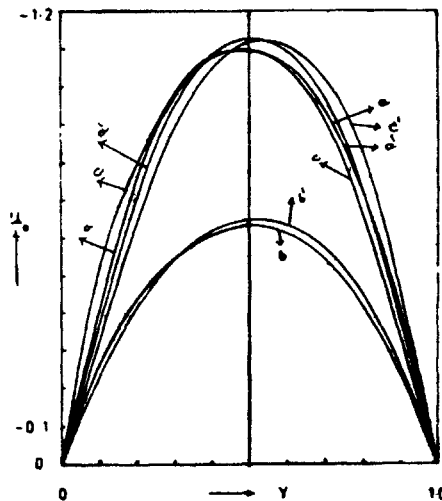


FIG. 1 : Profiles for the zeroth order velocity (u_0)

	a	a'	b	b'	c	c'
M	1	1	3	3	1	1
S	0.2	-0.2	0.2	-0.2	0.4	-0.4

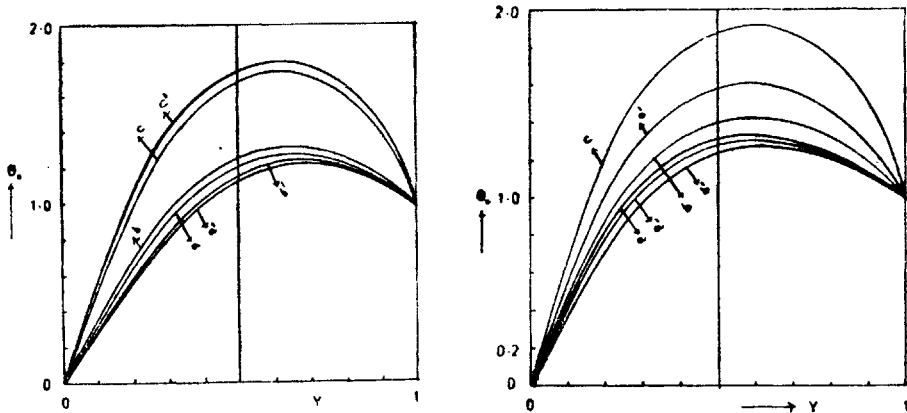


FIG. 2 : Profiles for the zeroth order temperature (θ_0) with $P = 0.71$.

	a	a'	b	b'	c	c'
M	1	1	1	1	1	1
S	0.2	-0.2	0.4	-0.4	0.2	-0.2
α	5	5	5	5	10	10

FIG. 3 : Profiles for θ_0 with $P = 7$ Curves as in Fig. 2.

temperature near the plane wall is rapid in compared to its growth when S is negative. This difference in the growth rates is much pronounced in case of air ($P = 7$). For an increase in $S (> 0)$ the temperature increase uniformly although the region while for an increase in $S (< 0)$ the temperature decrease throughout the channel. Whereas for fixed S (positive or negative) an increase in the heat parameter α increases the temperature w. r. t. an increase in α is much large in compared to its growth w.r.t. an increase in $S (> 0)$.

The perturbation in the axial velocity (u_1) (Figs. 4, 5) contributes to the growth of the total axial velocity in region I and retards the same in the region II. This perturbation has a steep rise near the plane wall and a similar fall near the wavy boundary. The maximum in either region is attained very near the boundary. In the region I it rapidly falls from its maximum value to the lowest value near the mid plane and once again rises in a narrow strip adjacent the mid plane before getting reversed in the region II. This u_1 contributes to the fluid acceleration along the channel in the region I and retards the motion in the region II. For all the values of the governing parameters, the extremes of the total axial velocity occur very near the boundaries the minimum value being near the wavy wall. For an increase in the wave length (λ) the growth in the magnitude of u_1 is almost proportional to variation in λ . When the suction (or injection) rate is maintained, an increase in the Hartmann number decreases the positive perturbations in region I and increases the reversed flow magnitudes in region II. Thus the axial motion is

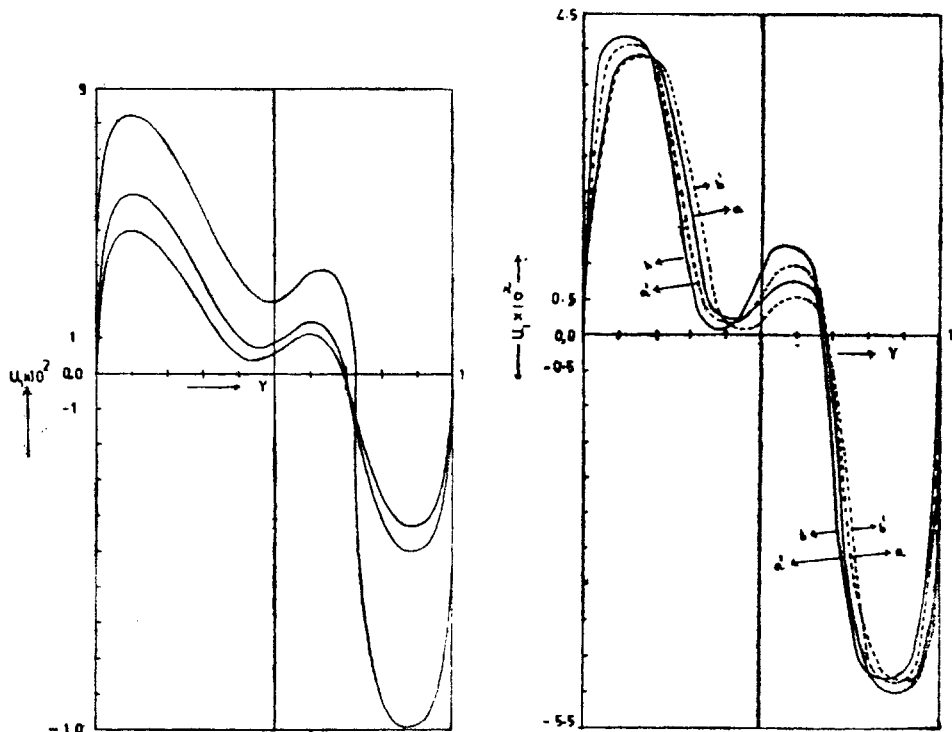


FIG. 4 : First order axial velocity (u_1) with $S = 0.2, \alpha = 5$

	a	b	c
M	1	1	1
λ	0.01	0.02	0.01

FIG. 5 : Variation of u_1 for different S with $M = 1, \lambda = 0.01$

	a	a'	b	b'
S	0.2	-0.2	0.4	-0.4

retarded in general due to an increase in M . For a fixed M , an increase in $S (> 0)$, decreases the magnitude of the perturbations in region I and increases their magnitude in region II away from the boundaries. Thus the total axial velocity retards in general, except in a narrow layer abetting the boundary, due to an increase in the suction parameter. When S increases through negative values the reversal is true and hence the axial velocity grows everywhere except near the boundary layers.

The profiles for the induced transverse velocity v_1 (Figs. 6, 7) are asymmetric bell shaped curves with peaks attaining in the region II and v_1 is negative, for all values of the governing parameters. For fixed S and λ , an increase in M reduces the transverse velocity everywhere in the fluid region except in a narrow layer near

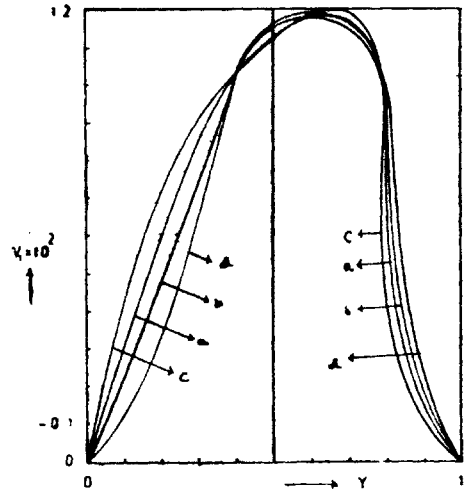
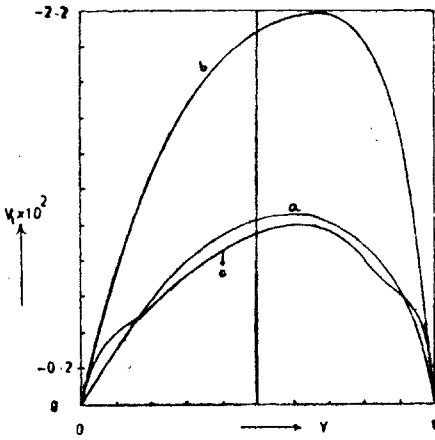


FIG. 6 : Variation of V_1 with $S = 0.2$ and $\alpha = 5$ Curves in Fig. 4.

FIG. 7 : Variation of (V_1) with S for $M = 1, \lambda = 0.01$. Curves as in Fig. 5.

the boundaries. Thus the effect of wavyness is to induce reversed transverse velocity whose peak values are attained near in the mid plane in the region II. v_1 rises in proportion to rise in the wave length λ . Also w.r.t. an increase in $S(> 0)$ and for a fixed M , v_1 is found to experience a depression near the mid plane with rise and fall towards the boundaries. In fact it rises near the plane wall to a certain extent and decreases towards the mid plane and later rises in region II before decaying towards the wavy wall. When S is negative, the reversal is true with an elevation in the mid plane.

The perturbed temperature θ_1 depends on M, λ, P, S and α the profiles are drawn for variations in these governing parameters (Figs. 8, 9, 10, 11). It is to be noted that θ_1 is negative for all variations in the parameters. The profiles for the perturbed temperature θ_1 are also asymmetric bell shaped curves with their peaks on the mid plane except in the case of large values of heat source parameter α . Keeping $\lambda, P, S, (> 0)$ and α fixed an increase in M , θ_1 increases although the region almost uniformly. For fixed M, S and λ , in case of water ($P = 0.71$) (Figs. 8, 9) θ_1 decreases in the region I and increases in the region II, for an increase in the heat source parameter α . In case of air ($P = 7$) (Figs. 10, 11) θ_1 decreases in a narrow layer near the plane wall and later increases although the region. This perturbed temperature θ_1 is found to decrease although the region for an increase in S either through positive or negative values for $P = 7$. However, in case of water it increase in region I to a certain extent and later decreases with an increase in $S(> 0)$. This behaviour gets reversed for an increase in $S(< 0)$. In general the effect of wavyness is to reduce the total temperature in the entire flow field. This

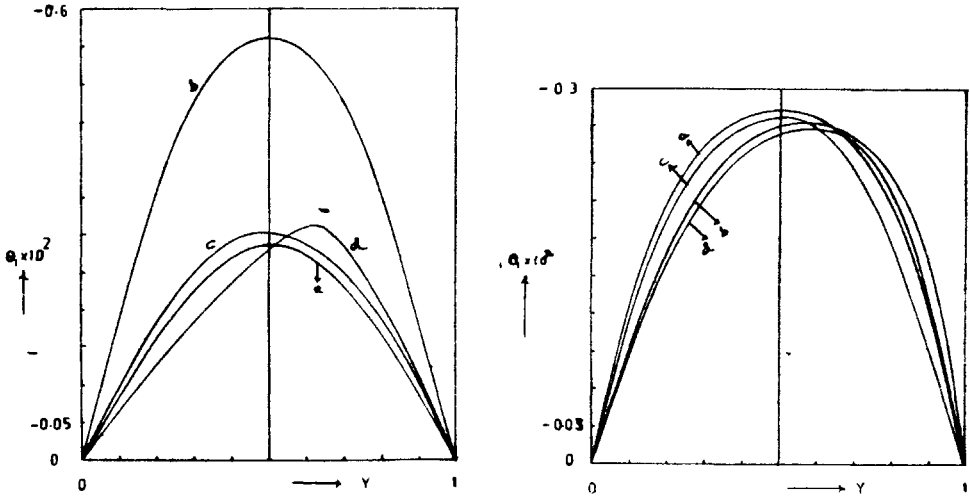


FIG. 8 : Profiles for the first order temperature distribution (θ_1) with $P = 0.71$.

	a	b	c	d
M	1	1	3	1
λ	0.01	0.02	0.01	0.01
α	5	5	5	10

FIG. 9 : Variation of θ_1 for different S for $M = 1, \lambda = 0.01, \alpha = 5$.

	a	b	c	d
S	0.2	-0.2	0.4	-0.4

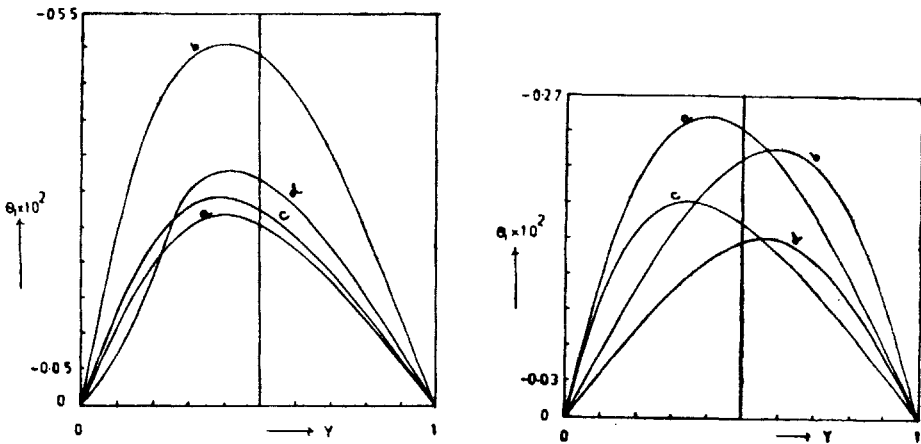


FIG. 10 : Variation of θ_1 , when $S = 0.2$ and $P = 7$.

Curves as in Fig. 8.

FIG. 11 : Variation of θ_1 with S for $M = 1, \lambda = 0.01, \alpha = 5$.

Curves as in Fig. 9.

TABLE I
Skin friction at the plane wall (τ_0)

$S \backslash \tau_0$	$M = 1$	$M = 3$
0.2	-0.8475	-0.6879
-0.2	-0.8114	-0.6659
0.4	-0.8655	-0.6990
-0.4	-0.7936	-0.6552

TABLE II
Skin friction at the wavy wall (τ_1)

$S \backslash \tau_1$	$M = 1$	$M = 3$
0.2	0.09979	-0.07464
-0.2	0.1281	-0.05062
0.4	0.08578	-0.06884
-0.4	0.1423	-0.05676

reduction is more pronounced in the middle region of the channel compared to the boundary regions. A marginal increase in the magnetic parameter increases the decay of the total temperature to a little extent. Also this decay in the total temperature is found to vary for different variations in S , in both the cases of water and air.

The skin friction and the Nusselt number at plane and wavy walls are tabulated for variations in the governing parameters in Tables I-IV. On either of the boundaries the skin friction is found to decrease for an increase in M , keeping S fixed. But when M is fixed, an increase in $S(> 0)$ increases the skin friction at the plane wall while it is found to decrease for an increase in $S(< 0)$. At the wavy wall, the skin friction is found to decrease for an increase in $S(> 0)$ and increase for an increase in $S(< 0)$. Also it can be observed that the magnitude of the skin friction at the plane wall is very much large compared to its magnitude of the wavy wall. This shows that the effect of the wavyness is to reduce the skin friction on the boundaries to a very large extent. The Nusselt numbers at the boundaries almost do not vary for small variations in the magnetic parameter. The Nusselt numbers is found to decrease for an increase in $S(> 0)$ for all M , α and P . However, its behaviour w.r.t. an increase in $S(< 0)$ depends on α . A similar behaviour is found w.r.t. variations in λ . At the plane wall the Nusselt number (in case of water and air) increases with an increase in M or $S(> 0)$. But it decreases with an increase in $S(< 0)$ for all M and P .

TABLE III
Nusselt Number (N_0) at the plane wall

$\alpha \setminus N_0$	a		a'		b		b'		c		c'		d		d'	
	$P=0.71$	$P=7$	$P=0.71$	$P=7$	$P=0.71$	$P=7$	$P=0.71$	$P=7$	$P=0.71$	$P=7$	$P=0.71$	$P=7$	$P=0.71$	$P=7$	$P=0.71$	$P=7$
0	1.018	1.863	0.936	0.462	1.078	1.863	0.93	0.462	1.154	2.984	0.87	0.187	1.154	2.97	0.854	0.17
5	3.623	4.908	3.364	2.39	3.623	4.908	3.364	2.39	3.757	6.499	3.24	1.643	4.131	2.96	3.543	1.93
10	6.168	7.954	5.792	4.317	6.168	7.954	5.792	4.319	6.361	10.01	5.609	3.101	6.917	11.24	6.25	4.05
M	1	1	1	3	1	3	1	3	1	1	1	1	1	1	1	1
S	0.2	-0.2	-0.2	0.2	0.2	0.2	-0.2	-0.2	0.4	0.4	-0.4	-0.4	0.4	0.4	-0.4	-0.4
λ	0.01	0.01	0.01	0.01	0.01	0.01	0.01	0.01	0.01	0.01	0.01	0.01	0.02	0.02	0.02	0.02

TABLE IV
Nusselt Number (N_1) at the wavy wall

$\alpha \setminus N_1$	a		a'		b		b'		c		c'		d		d'	
	$P=0.71$	$P=7$	$P=0.71$	$P=7$	$P=0.71$	$P=7$	$P=0.71$	$P=7$	$P=0.71$	$P=7$	$P=0.71$	$P=7$	$P=0.71$	$P=7$	$P=0.71$	$P=7$
0	0.93	0.454	1.074	1.872	0.93	0.4548	1.074	1.872	0.863	0.178	1.151	3.036	0.883	5.76	1.127	2.83
5	-1.563	-1.52	-1.542	-1.27	-1.563	-1.15	-1.497	-1.12	-1.569	-1.32	-1.526	-0.62	-1.389	-1.93	-1.056	-2.5
10	-4.056	-3.49	-4.157	-4.41	-4.056	-3.49	-4.157	-4.41	-4.001	-2.81	-4.202	-4.27	-3.651	-4.03	-3.243	-11.1

ACKNOWLEDGMENT

We are thankful to Dr D V Krishna, S K University, Anantapuri for his valuable suggestions in the preparation of this paper. One of the authors (R Sivaprasad) is thankful to C.S.I.R., New Delhi for awarding a Junior Research Fellowship.

REFERENCES

1. T F Gaskell, *The Earth's Mantle*, New York, Academic Press (1967).
2. S K Runcorn, *Nature* **195** (1962) 1248.
3. D C Tozer, *Proc. R. Soc. A.* **58** (1966) p. 251.
4. H A Bethe, *Science* **161** (1968) 541.
5. R B Bird, *J. Soc. Plastic Engns.* **11** (7) (1955).
6. R M Inman, *Int. J. Heat Mass Transfer* **5** (1962) 1053.
7. S Ostrach, *NACA, TN.* (1952) 2863.
8. H F Poppendick, *Chem. Eng. Symp. Ser.* **50** (11) (1954) 93.
9. K S Sastri, Doctoral thesis, I.I.T. Kharagpur (1964).
10. P L Chambre, *Appl. Sci. Res., Sec. A,* **6** (1957) 393.
11. W N Gill, *J. Amer. Inst. Chem. Engns.* **8** (1962) 137.
12. R J Grosh and R D Cess, *Trans. Amer. Soc. Mech. Engns.* **80** (1958) 667.
13. S K Helmann, G Habeller, and H Babrov, *Trans. Amer. Soc., Mech., Engns.* **78** (1956) 1155.
14. G M Low, *J. Aero Sci.* **22** (1955) 329.
15. R E Gee and J B Lyon, *Industry Engg. Chem.* **49** (1957) 596.
16. J Modejskii, *Int. J. Heat mass Transfer* **6** (1963) 49.
17. I V Kragelskii, *Friction and Wear*, Butterworths, London (1965).
18. S G Lekeoudis, A M Nayfeh, and W S Saric, *Phys. fluids* **19** (1976) 514.
19. P N Sankar and U N Sinha, *J. Fluid Mech.* **77** (1976) 243.
20. K Vajravelu and K S Sastri, *J. Fluid Mech.* **86** (2) (1978) 365.
21. D R V Prasada Rao, D V Krishna and L Debnath, *Int. J. Engg. Sci. V.* (1983) 21.

APPENDIX

$$a_1 = (m \sinh m - S/2 \cosh m) \exp(-S/2)$$

$$a_2 = (m \cosh m - S/2 \sinh m) \exp(-S/2)$$

$$a_3 = \exp(-S/2 \cosh(m)) \quad a_4 = \exp(-S/2 \sinh(m))$$

$$a_{47} = (a_3 - 1 + S/2)(a_2 - m)(a_1 + S/2)(a_4 - m)$$

$$A_1 = u'_0(1)(a_4 - m)/a_{47}$$

$$A_3 = -A_1$$

$$A_4 = u'_0(1)(a_3 - 1 + S/2)/a_{47}$$

$$A_2 = S/2 A_3 - mA_4$$

$$a_5 = (m^2 + S^2/4)$$

$$a_6 = mS$$

$$a_{42} = m^2 + S/2$$

$$a_7 = a_4 \exp(S/2)$$

$$a_8 = -m(1 + S/2) \exp(S/2)$$

$$a_9 = a_{42}A_3 - a_8A_4$$

$$a_{10} = a_{42}A_4 - a_6A_3$$

$$a_{11} = \frac{c}{M^2} \left(\frac{a_9}{\sinh m} - a_5A_3 \right)$$

$$a_{12} = \frac{c}{M^2} \left(\frac{a_{10}}{\sinh m} - a_5A_4 \right)$$

$$a_{43} = ca_5/M^2$$

$$a_{44} = ca_6/M^2$$

$$a_{45} = ca_7/M^2$$

$$a_{46} = ca_8/M^2$$

$$a_{13} = a_{43}A_1$$

$$a_{14} = a_{43}A_2$$

$$a_{15} = a_{44}A_1$$

$$a_{16} = a_{44}A_2$$

$$a_{17} = a_{44}A_3$$

$$a_{18} = a_{44}A_4$$

$$a_{19} = \frac{c}{M^2} \left(a_8A_4 - a_7A_3 - \frac{a_9(\exp S/2)}{\sinh m} \right)$$

$$a_{20} = a_{45}A_4$$

$$a_{21} = a_{45}A_1$$

$$a_{22} = a_{45}A_2$$

$$a_{23} = a_{46}A_3$$

$$a_{24} = a_{46}A_1$$

$$a_{25} = a_{46}A_2$$

$$b_8 = m - S/2$$

$$b_9 = m + S/2$$

$$a_{26} = (m + 1)S/2$$

$$a_{27} = (m^2 \cosh m - mS \sinh m + S^2/4 \cosh m) \exp(-S/2)$$

$$a_{28} = (m^2 \sinh m - mS \cosh m + S^2/4 \sinh m) \exp(-S/2)$$

$$c_2 = (1 + a_{40}) (\exp(-PS) - 1)$$

$$c_4 = \theta'_0(1)/(1 - \exp(-SP))$$

$$a_{41} = PS c_2$$

$$a_{31} = cc_4/M^2$$

$$a_{29} = a_{31}/\sinh m$$

$$a_{30} = a_{29} \exp(S/2)$$

$$a_{32} = a_{41}A_1$$

$$a_{33} = a_{40}A_1$$

$$a_{34} = a_{41}A_2$$

$$a_{35} = a_{40}A_2$$

$$a_{36} = a_{41}A_3$$

$$a_{37} = a_{40}A_3$$

$$a_{38} = a_{41}A_4$$

$$a_{39} = a_{40}A_4$$

$$b_1 = 2b_8^2 (b_8^2 + Sb_8 - M^2)$$

$$b_2 = 2b_9^2 (b_9^2 - Sb_9 - M^2)$$

$$b_3 = 16b_8^2 (4b_8^2 + 2Sb_8 - M^2)$$

$$b_4 = 16b_9^2 (4b_9^2 - 2Sb_9 - M^2)$$

$$b_5 = \frac{4b_8^2 + 3Sb_8 - 2M^2}{b_8(b_8^2 + Sb_8 - M^2)}$$

$$b_6 = \frac{4b_9^2 - 3Sb_9 - 2M^2}{b_9(b_9^2 - Sb_9 - M^2)}$$

$$b_7 = 8S^2M^2$$

$$d_1 = [\exp(-m) ((a_{14} - a_{16})b_5 + (a_{15} - a_{13})) - c(a_9 - a_{10})/M^2 \\ + (a_{21} + a_{24}) - (a_{22} + a_{25})b_5]b_1$$

$$d_2 = [\exp(-m) (a_{11} - a_{16}) - a_{25} - a_{22}]/b_1$$

$$d_3 = [\exp(m) (a_{13} + a_{15} + (a_{14} + a_{16})b_6) - c(a_9 + a_{10})/M^2 \\ - a_{21} + a_{24} + (a_{25} - a_{22})b_5]/b_2$$

$$d_4 = [\exp(m) (a_{14} + a_{16}) + (a_{25} - a_{22})]/b_2$$

$$d_8 = (c a_{10} \exp(S/2)/M^2 \sinh m + a_{20} + a_{21})$$

$$d_5 = [\exp(-m) (a_{11} + a_{12} + a_{17} + a_{18}) - a_{19} - d_8]/b_3$$

$$d_6 = [\exp(m) (a_{11} - a_{12} - a_{17} + a_{18}) - a_{19} - d_8]/b_4$$

$$d_7 = [\cosh(m) (a_{12} - a_{17}) + \sinh m (a_{11} + a_{18}) - d_8]/b_7$$

$$\phi_1(y) = (d_1 - d_2y) \exp(b_8y) + (d_3 + d_4y) \exp(-b_9y) \\ + d_5 \exp(2b_8y) - d_6 \exp(-2b_9y) + d_7 \exp(-Sy)$$

$$B_3 = c_5/a_{47}$$

$$B_4 = (\phi'_1(0) - \phi'_1(1) - B_3(a_1 + S/2))/(a_2 - m)$$

$$B_1 = -\phi(0) - B_3$$

$$B_2 = -a_1B_3 - a_2B_4 - \phi'_1(1)$$

$$c_5 = (\phi'_1(1) - \phi'_1(0))(a_4 - m) - (a_2 - m)(\phi_1(1) - \phi(0) - \phi'(0))$$

$$d_{11} = (a_{29} \exp(-m) - (a_{30} + a_{38} + a_{36}))/b_{13}$$

$$d_{12} = (a_{29} \exp(m) - (a_{30} + a_{38} - a_{36}))/b_{14}$$

$$d_{13} = (a_{29} \exp(-m) - (a_{30} - a_{39} - a_{37}))/b_{15}$$

$$d_{14} = (a_{29} \exp(m) - (a_{30} - a_{39} + a_{37}))/b_{16}$$

$$d_{15} = a_{31} + a_{38}$$

$$d_{16} = (a_{31} - a_{32})PS - a_{34}/P^2S^2$$

$$d_{17} = a_{34}/2PS$$

$$d_{18} = a_{34}/(PS)^2$$

$$d_{19} = a_{35}$$

$$\phi_2(y) = P [d_{11} \exp(b_8 - PS)y - d_{12} \exp(-(b_9 PS)y) \\ - a_{13} \exp(b_8y) + (d_{17}y^2 + d_{18}y - d_{16}) \exp(-PS)y \\ + d_{13} \exp(-b_9y) - d_{15} - a_{25}y]$$

$$D_2 = (\phi_2(0) - \phi_2(1))/(\exp(-PS) - 1)$$

$$D_1 = -D_2 - \phi_2(0)$$